Biosensors and Bioelectronics 24 (2008) 306–312

Contents lists available at ScienceDirect

Biosensors and Bioelectronics

journal homepage: www.elsevier.com/locate/bios

Highly sensitive biosensor based on bionanomultilayer with water-soluble multiwall carbon nanotubes for determination of phenolics

Lijun Liu [1], Fu Zhang, Fengna Xi, Xianfu Lin *

Department of Chemistry, Zhejiang University, Hangzhou 310027, PR China

ARTICLE INFO

Article history:
Received 23 January 2008
Received in revised form 3 April 2008
Accepted 3 April 2008
Available online 12 April 2008

Keywords:
Biosensor
Multiwall carbon nanotubes (MWNTs)
Barbiturates
Bionanomultilayer
Phenolics

ABSTRACT

A highly sensitive biosensor was developed based on bionanomultilyer with water-soluble carbon nanotubes (CNTs). The water-soluble poly(allylamine hydrochloride)-wrapped multiwall carbon nanotubes (PAH-MWNTs) can be obtained for the first time relying on the function of barbiturates, which provides a useful avenue for CNT application in material science and biosensor technology. Based on this, the PAH-MWNTs/horseradish peroxidase (HRP) bionanomultilayer was prepared via layer-by-layer (LBL) assembly. Electrochemical impedance spectroscopy, atomic force microscopy and UV–vis spectra were adopted to monitor the uniform LBL assembly of the homogeneous bionanomultilayer. The bionanomultilayer was used to construct a phenolic biosensor. Under the optimal conditions, the biosensor presented a linear response for catechol from 0.1 to 20.4 μM, with a detection limit of 0.06 μM. A series of phenolics were detected by the bionanomultilayer biosensor. The introduced MWNTs in the biosensor provided a suitable microenvironment to retain the HRP activity and acted as a transducer for amplifying the electrochemical signal of the product of the enzymatic reaction. So the developed bionanomultilayer biosensor exhibited a fast, sensitive and stable detection.

1. Introduction

Electrochemical biosensor has been used in a broad field ranging from clinical diagnostics to environmental analysis. The suitable electrochemical material used for immobilizing biomolecules plays a key role in construction of biosensors. Carbon nanotubes (CNTs) represent a new class of nanomaterials that possess high surface area, unique electronic, thermal and mechanical properties, and high aspect ratios (Ajayan, 1999; Baughman et al., 2002). The excellent biocompatibility and capability to improve the electron transfer make them extremely attractive for applying to electrochemical biosensors (Cosnier, 2003; Sampath and Lev, 1996; Wang, 2005; Wang and Musameh, 2003; Zhang et al., 2004; Zhao et al., 2002). For example, the biosensors based on the matrix of CNTs/3-aminopropyltriethoxysilane composite to cross-link organophosphorus hydrolase (Deo et al., 2005), CNTs-chitosan composite for detection of 2,2′-azino-bis-(3-ethylbenzthiazoline-6-sulfonic acid) diammonium salt, catechol and O_2 (Liu et al., 2006).

However, a major barrier for the preparation of CNT-based biosensors is the poor dispersability of CNTs in most solvents (Pompeo and Resasco, 2002; Star et al., 2002). To suspend CNTs in solvents, especially in water, considerable efforts have been made. The application of organic solvent is limited because the residual organic solvents may denature biological molecules (Wu et al., 2002; Yan et al., 2004). The chemical modification with hydrophilic substances can improve the solubility of CNTs in water. But the method can perturb their intrinsic properties (Chen et al., 1998; Georgakilas et al., 2002). Since O'Connell et al. (2001) first reported the solubilization of single-wall carbon nanotubes (SWNTs) in water by noncovalently associating them with linear polymers such as polyvinyl pyrrolidone (PVP) and polystyrene sulfonate (PSS), this solubilizaton process has opened the door to introduce pristine CNTs into biosensor system. Wang et al. reported the ability of the perfluorosulfonated polymer Nafion to solubilize CNTs and constructed a CNT/Nafion biosensor (Wang and Musameh, 2003). A hydrogen peroxide biosensor was developed by Chen and Lu (2007), which was based on the encapsulation of hemoglobin (Hb) in the composite film of carboxylic CNTs and polyelectrolyte-surfactant (CTAB-PSS) polymer. Ali et al. took advantage of the poly(anilineboronic acid) (PAA)/CNT composite and the ion-exchange polymer Nafion to construct a sensitive and selective neurotransmitter dopamine biosensor (Ali et al., 2007). All in all, the CNTs wrapped with polymer exhibit promising potential in the realm of electrochemical biosensor.

In this paper, the water-soluble poly(allylamine hydrochloride)-wrapped MWNTs (PAH-MWNTs) were obtained for the first time

* Corresponding author. Tel.: +86 571 87951588; fax: +86 571 87952618.
E-mail address: llc123@zju.edu.cn (X. Lin).
[1] Address: School of Chemistry and Chemical Engineering, Jinggangshan University, Ji'an, 343009, PR China.

0956-5663/$ – see front matter © 2008 Elsevier B.V. All rights reserved.
doi:10.1016/j.bios.2008.04.003

relying on the function of the barbiturates, which provides a useful avenue for CNT application in material science and biosensor technology. Using horseradish peroxidase (HRP) as a model enzyme, the $(PAH\text{-}MWNTs/HRP)_n$ bionanomultilayer was prepared on the Au electrode through layer-by-layer (LBL) assembly and used for a biosensor construction to determine a series of phenolics. The introduced MWNTs in the biosensor played a dual significant role in both the enzyme immobilization and transduction events, which provided a suitable microenvironment to retain the HRP activity and acted as a transducer for amplifying the electrochemical signal of the product of the enzymatic reaction. So the developed bionanomultilayer biosensor exhibited a fast, sensitive and stable detection.

2. Experimental

2.1. Materials

Poly(allylamine hydrochloride) (PAH, MW 15 000) and poly(sodium-*p*-styrene-sulfonate) (PSS, MW 70 000) were both obtained from Aldrich. HRP (E.C. 1.11.1.7, 250 U mg^{-1}, p*I* 7.2) was purchased from Shanghai Dongfeng biotechnology Co. Ltd., China. 3-mercapto-1-propanesulfonic acid, sodium salt (MPS) was purchased from Acros. All other chemicals were of analytical grade and used without further purification. Doubly distilled water was used throughout the work.

The multiwall carbon nanotubes (95%, MWNTs) and single-wall carbon nanotubes (75–80%, SWNTs) (from Shenzhen Nanotech. Port. Co., Ltd., Shenzhen, China) were purified by refluxing in 3 M nitric acid for 12 h. The solution was transferred to polytetrafluoroethylene centrifuge tubes and spun at 2400 × *g* for 2 h (Liu et al., 1998). The supernatant acid was decanted off. The resultant solid was ultrasonicated in concentrated HNO_3 and H_2SO_4 (volume ratio of 1:3) for 6 h followed by extensive washing and filtrating in deionized water until the filtrate was neutral. Then the pH was adjusted to 8.0 to achieve net negatively charged carboxylate anions (Liu and Lin, 2006). The negatively charged MWNTs were centrifuged at 14 000 × *g* for 30 min to remove the supernatant and dried in a vacuum at 50 °C. The carboxylate CNTs were dispersed in 0.04 M barbiturates with 1 min ultrasonication to obtain the required suspension. The PAH-MWNTs were prepared by adding 1 mg ml^{-1} PAH into 1 mg ml^{-1} MWNT suspension.

2.2. Preparation of PAH-MWNTs/HRP bionanomultilayer

The Au electrode (0.5 cm × 1.0 cm) was successively polished with emery paper and alumina slurry of 0.05 μm, and rinsed with pure water with ultrasonication assistance. Then it was soaked in freshly prepared Piranha solution (30% H_2O_2 and concentrated H_2SO_4, 1:3 v/v) at 80 °C for 30 min. After being sonicated in deionized water, the clean electrode was electrochemically pre-treated by cyclic potential scanning between 1.4 and −0.2 V in H_2SO_4 (0.2 M) until the cyclic voltammogram characteristic was stable. The stable Au electrode was immersed in a 0.02 M MPS solution for 10 h to form a monolayer of negative charge. PET film (1.0 cm × 1.0 cm) was first dipped in methanol for 30 min and washed with water. Then it was soaked in 15% (m/v) NaOH solution for about 4 h, followed by a rinse in diluted hydrochloric acid and water, and dried with nitrogen stream.

PAH and PSS solutions of 1 mg ml^{-1} in pH 12.0 glycine–NaOH buffer containing 0.4 M NaCl were prepared. Precursor of PAH/PSS was assembled on MPS-modified Au electrod and PET film by dipping them into the PAH and PSS solutions for 20 min. After each adsorption step, the modified electrode was thoroughly rinsed with distilled water. The LBL assembly $(PAH\text{-}MWNTs/HRP)_n$ bionanomultilayer was formed by sequential deposition of PAH-MWNTs and HRP on the precursor films. The MWNT and HRP solutions were 1 mg ml^{-1} in 0.04 M barbital buffer at pH 9.0 and 8.0, respectively. After each deposition cycle, samples were rinsed with water for 2 min and then dried with nitrogen.

2.3. $(PAH\text{-}MWNTs/HRP)_n$ bionanomultilayer characterization

The PAH-MWNTs suspension was loaded on a carbon-coated 200 mesh copper grid and observed under a transmission electron microscope (TEM, JEM 200CX) at 100 kV electron beam accelerating voltage. Typically, 25 μl of the suspension was dropped on the grid, and the extra solution was then allowed to air-dry.

Atomic force microscopy (AFM) image was performed by Nanoscope IVa (Digital Instruments/Veeco Metrology Group, USA) in tapping mode. 30 μl of the PAH-MWNTs and HRP were alternated onto a freshly cleaved mica surface until the required bionanomultilayer was obtained. The samples were then air-dried and analyzed by AFM.

UV–vis absorption measurements were taken using a Shimadzu UV-2550 spectrophotometer. The activity of HRP in the bionanomultilayer on PET film was determined by Worthington method (Jiang et al., 2004). A mixture of 0.2 ml fresh H_2O_2 solution and 0.2 ml color reagent consisting of 0.5 mg ml^{-1} 4-amino antipyrine and 16 mg ml^{-1} phenol in pH 7.0 PBS was added into a microcuvette. The cuvette was warmed up 10 min in water bath at 37 °C, inserted a multilayer PET film. After stirred at 37 °C for 5 min, the film was taken out, and the spectra of the remained solution was obtained from 350 to 700 nm by UV–vis.

2.4. Electrochemical measurement

Cyclic voltammetry and amperometric experiments were carried out on a CHI 650C electrochemical workstation (CH Instruments, USA). A conventional three-electrode electrochemical cell was used with a platinum disk electrode as the auxiliary electrode, an Ag/AgCl electrode saturated with KCl as the reference electrode and a modified Au electrode as the working electrode. The supporting electrolytes were 5 mM $K_3[Fe(CN)_6]/K_4[Fe(CN)_6]$ (1:1) mixture for cyclic voltammetry and 0.2 M phosphate buffer solution (PBS) for amperometric experiments.

3. Results and discussion

3.1. The solubilization of PAH-MWNTs

Both of the carboxylate MWNTs and SWNTs can be easily solubilized in barbital solution while the noncarboxylate CNTs cannot. The interesting phenomenon led us to carry out farther investigation. Other barbiturates such as barbituric acid and amobarbital were chosen to disperse CNTs and the same results were obtained. Barbital buffers are the commonly used buffer systems for biological and biomedical research. Thus, it was chosen as a typical example for further study. The MWNTs can be solubilized in barbital buffer at pH 7.0–9.0. The soluble MWNTs in pH 9.0 barbital buffer were used to prepare PAH-wrapped MWNTs (PAH-MWNTs). The MWNT solution still remained a homogenous state after adding the polycation PAH. Fig. 1A displays the comparison of PAH-MWNTs dispersing in 0.04 M barbital (1) and in water (2). It is clear that without the help of the barbital, PAH do not disperse or wrap MWNTs. TEM image of PAH-MWNTs indicates the tubes are hollow and wrapped by PAH layer (Fig. 1B). The thickness of PAH layer is about 5 nm. Based on above results, it is proposed that the alkalescence of the barbiturates and the acidity of the CNTs

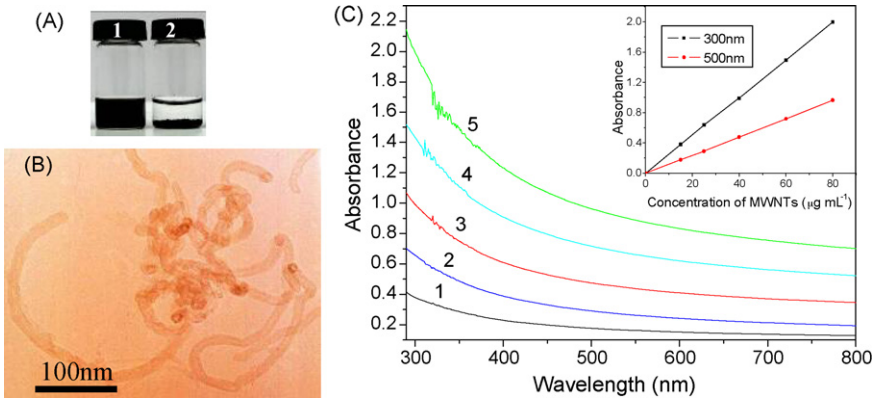

Fig. 1. (A) Dispersions of 1 mg ml^{-1} MWNTs in 0.4 M barbital (1) and in water (2), with adding 1 mg ml^{-1} PAH. (B) TEM image of the PAH-MWNTs in 0.04 M barbital solutions. (C) UV–vis absorption spectra of PAH-MWNTs of different concentrations: (1) 0.015 mg ml^{-1}; (2) 0.025 mg ml^{-1}; (3) 0.040 mg ml^{-1}; (4) 0.060 mg ml^{-1}; (5) 0.080 mg ml^{-1} in pH 9.0 barbital–HCl buffer with adding 1 mg ml^{-1} PAH. Inset: Calibration curves of the absorbance at 300 and 500 nm vs. MWNT concentration.

terminated with carboxylate groups result in a CNT-barbiturate zwitterions which leads to the solubilization of CNTs in absolute aqueous solution (see step 1 of Scheme 1). The cations of barbiturates in the CNT-barbiturate zwitterions can be readily exchanged by the positively charged PAH. So the water-soluble PAH-MWNTs can be obtained. Fig. 1C is the UV–vis spectra of PAH-MWNTs at a wide range of concentrations in pH 9.0 barbital buffer. The dependence of absorbance on concentration at 300 and 500 nm obeys Beer's law (Fig. 1C, inset), which could be associated with concentration-dependent MWNT aggregation. It indicates that PAH-MWNTs dispersed by barbitals keep the pristine features. The UV–vis spectra of PAH-MWNTs consisting of different PAH concentrations are almost the same (not shown). The independence of UV–vis spectra of solution on PAH concentration demonstrates that the observed absorbances are from MWNTs rather than PAH. Such features can serve as the basis for developing bionanomultilayer of CNTs.

3.2. *The assembly and characterization of (PAH-MWNTs/HRP)$_n$ bionanomultilayer*

As shown in step 2 of Scheme 1, PAH-MWNTs have positive charges due to PAH as the outmost layer. HRP, which has an isoelectric point of pH 7.2, possesses net positive charges at pH 8.0.

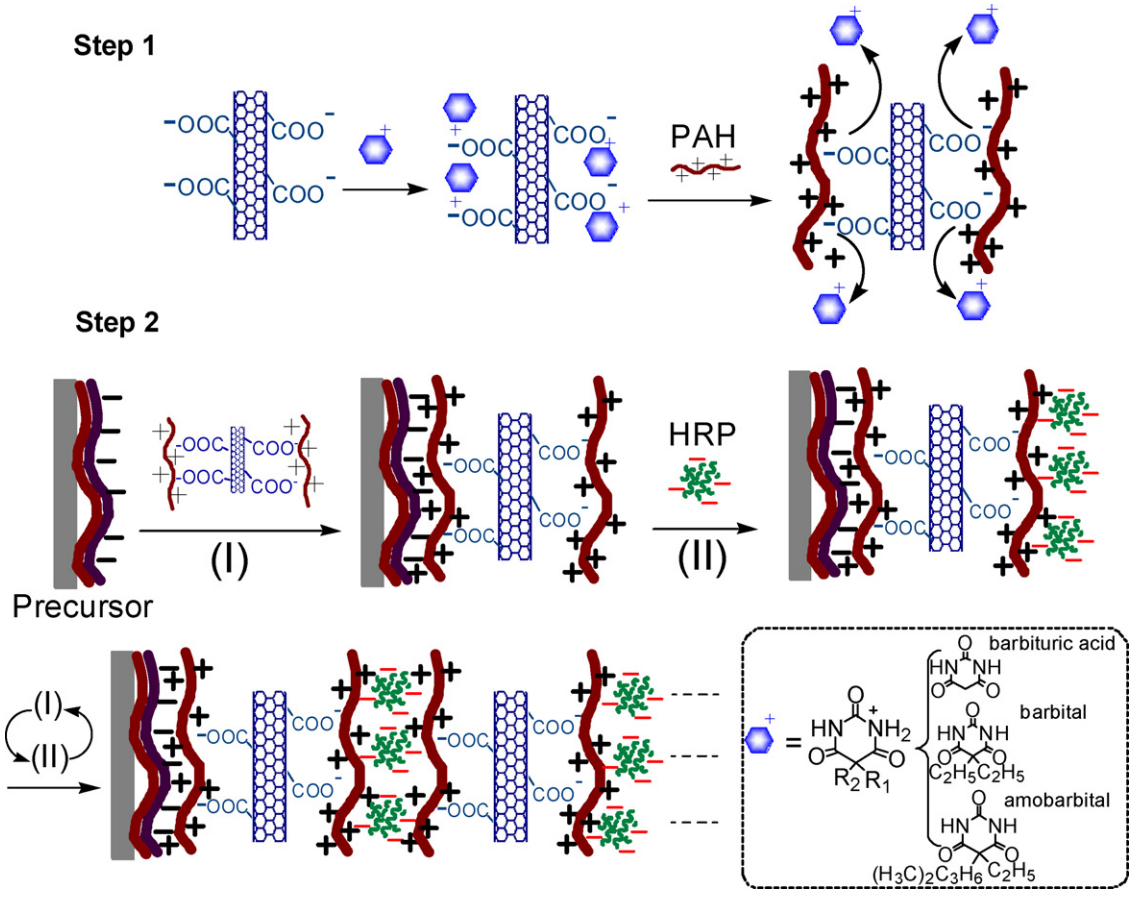

Scheme 1. The process of solubilizing PAH-MWNTs and assembly bionanomultilayer.

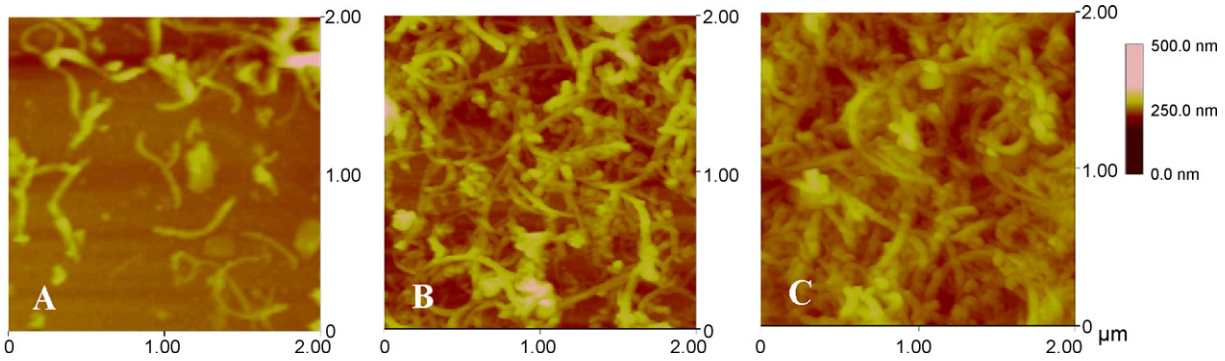

Fig. 2. AFM images of (A) PAH-MWNTs/HRP, (B) $(PAH\text{-}MWNTs/HRP)_5$ and (C) $(PAH\text{-}MWNTs/HRP)_9$ assembled onto the freshly cleaved mica surface.

PAH-MWNTs and HRP were alternatively and circularly adsorbed onto the precursor of PAH/PSS which formed on the anionized PET substrate. So the required $(PAH\text{-}MWNTs/HRP)_n$ bionanomultilayer was obtained through the LBL assembly technology.

The LBL assembly process was monitored by AFM (Fig. 2). When the first PAH-MWNTs/HRP bilayer assembled onto the freshly cleaved mica surface, the MWNTs are solely dispersed without wrapping with each other (Fig. 2A). Several spherical aggregates, probably corresponding to the accumulated enzyme molecules, are observed in the image. After the number of PAH-MWNTs/HRP bilayers increase to five, the MWNT coverage displays a dramatic increase (Fig. 2B). But there still exist interspaces on the surface. When nine bilayers are formed, the mica surface is fully covered by the uniform MWNT layer and the interspaces are hardly observed (Fig. 2C). It is confirmed that the LBL technology can produce a uniform film on the entire surface of the substrate.

3.3. *Electrochemical properties of the $(PAH\text{-}MWNTs/HRP)_n$ bionanomultilayer electrode*

The electrochemical impendence spectra (EIS) can offer the evidence of uniform deposition of the bionanomultilayer on Au electrode. The EIS consists of a semicircle portion observed at higher frequency range corresponding to the electron-transfer-limited process and a linear part at lower frequencies representing the diffusion-limited process. The diameter of the semicircle corresponds to the interfacial electron-transfer resistance (R_{ct}). Significant differences in the impedance spectra (Fig. 3A) were observed during stepwise formation of the PAH-MWNTs/HRP bionanomultilayer. Curves (a)–(e) of Fig. 3A are obtained at Au electrodes modified with precursor, PAH-MWNTs layer, PAH-MWNTs/HRP (one bilayer), five bilayers and nine bilayers, respectively. The values of the relevant R_{ct} are estimated to be 202, 45, 114, 617 and 1063 Ω, respectively. On the precursor (curve a of Fig. 3A), due to the electrostatic repulsion between the negatively charged PSS and probe molecule $Fe(CN)_6^{3-/4-}$ that blocked the interfacial charge transfer, there appeared a large semicircle corresponding to a large electron-transfer resistance. After adsorption of PAH-MWNTs, the positively charged surface accelerates the electron-transfer and results a lowest R_{ct} (curve b of Fig. 3A). With further assembly of HRP, the enzyme with negative charge blocks the access of the probe molecules to the electrode surface, and then the R_{ct} becomes larger (curve c of Fig. 3A). However, even if the film thickness becomes larger, the value of R_{ct} is less than that of the precursor film. It is attributed to the introduced MWNTs which promotes the electron transfer and increases the electrode surface. With the number of PAH-MWNTs/HRP bilayers increasing, the film on the electrode becomes thicker and thicker, and the interfacial charge transfer is more and more difficult (curve d, e of Fig. 3A). The values of R_{ct} increases proportionally to the number of the PAH-MWNTs/HRP bilayers, as shown in bottom inset of Fig. 3A. The result showed that PAH-MWNT/HRP bionanomultilayer was formed uniformly on the Au electrode.

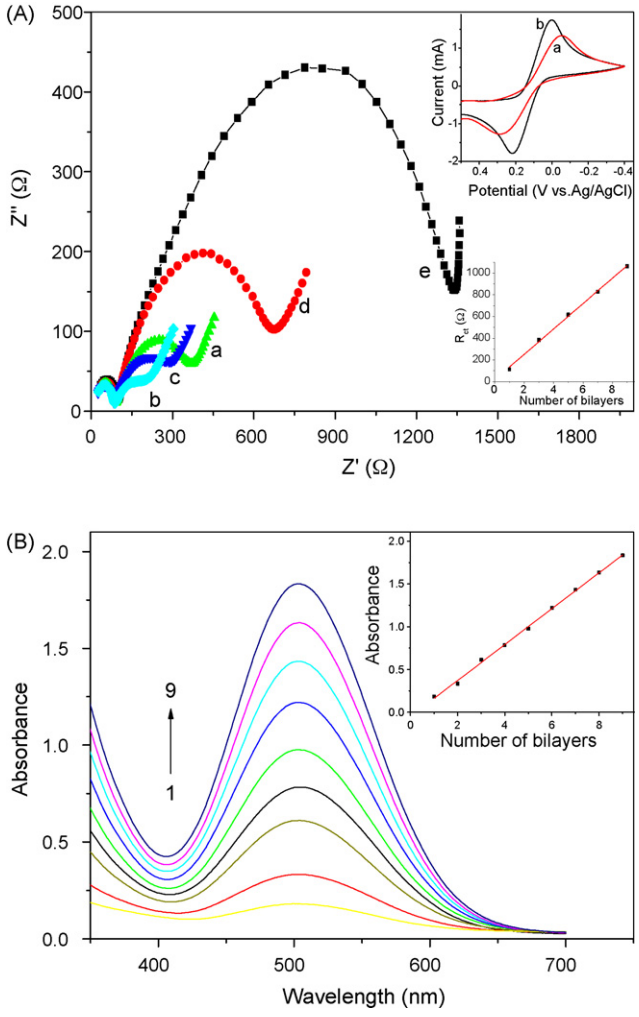

Fig. 3. (A) Electrochemical impedance spectra of the electrodes modified by different layers in 5 mmol L^{-1} $K_3[Fe(CN)_6]/K_4[Fe(CN)_6]$ (1:1) solutions: (a) MPS/PAH/PSS; (b) MPS/PAH/PSS/PAH-MWNTs, (c) MPS/PAH/PSS/(PAH-MWNTs/HRP) (one bilayer); (d) five bilayers; (e) nine bilayers. Bottom inset: relationship of R_{ct} vs. number of bilayers. Upper inset: the cyclic voltammograms of $Au/MPS/PAH/PSS/(PAH/HRP)_5$ electrode (a) and $Au/MPS/PAH/PSS/(PAH\text{-}MWNTs/HRP)_5$ electrode (b) in 5 mM $K_3[Fe(CN)_6]/K_4[Fe(CN)_6]$ (1:1) mixture. (B) UV–vis absorption spectra of one to nine bilayers of PAH-MWNTs/HRP. Inset: Calibration curve of the absorption at ~500 nm vs. the number of bilayers.

The electrochemical behavior at Au/MPS/PAH/PSS/$(PAH/HRP)_5$ and Au/MPS/PAH/PSS/$(PAH\text{-}MWNT/HRP)_5$ electrodes was studied by cyclic voltammetry taking $Fe(CN)_6^{3-/4-}$ as the probe as shown in upper inset of Fig. 3A. It is apparently that the peak current increases distinctly when MWNTs are introduced into the bionanomultilayer (curve b), whereas ΔE_p decrease as compared with that of no MWNT modified electrode (curve a). The higher peak current and decreased ΔE_p suggests that MWNTs improve the electron transfer, which agrees with the above results of impedance experiment.

Although thicker layers of assembled film can increase the electron transfer resistance and obstruct the diffusion of the substrate, but more enzymes can be fixed on the electrode and improve the sensitivity of the electrode, which have been confirmed by the UV–vis spectra through Worthington method. Worthington method is a reaction system of H_2O_2 and 4-amino antipyrine catalyzed by HRP (Jiang et al., 2004). Fig. 3B shows the UV–vis adsorption spectra of one to nine bilayers of PAH-MWNTs/HRP on PET film. The absorption at ~500 nm attributed to the red product of the reaction increases in proportion to the number of PAH-MWNTs/HRP bilayers (Fig. 3B, inset), which suggests a progressive and uniform assembly process of HRP. Taking into account above two factors, the bionanomultilayer containing five bilayers of PAH-MWNTs/HRP was selected for further investigation.

3.4. The characteristic of $(PAH\text{-}MWNTs/HRP)_n$ bionanomultilayer biosensor

3.4.1. The construction of the biosensor

On the electrode surface, HRP molecules are oxidized by hydrogen peroxide followed its reduction by phenolics. The reduction current is proportional to the phenolic concentration (Mello et al., 2003; Munteanu et al., 1998). Based on this, the $(PAH\text{-}MWNTs/HRP)_5$ modified electrode was developed to a biosensor for determination of phenolics. The conditions of the amperometric experiments were optimized. The response of the bionanomultilayer electrode increased sharply with the concentration of hydrogen peroxide. However, too high hydrogen peroxide concentration would cause active centers of enzyme occupied and lead to inhibition of the enzyme catalytic activity. So 40 μM hydrogen peroxide was used in the following experiments. To avoid interference at high negative applied potential, −0.15 V (versus Ag/AgCl) was selected for amperometric measurements. The effect of pH from 5.0 to 8.0 was also considered. The current response of the biosensor reached the highest point at pH 6.5. Under the optimized conditions, the comparison of the current response of the Au/MPS/PAH/PSS/$(PAH/HRP)_5$ (curve a) and Au/MPS/PAH/PSS/$(PAH\text{-}MWNTs/HRP)_5$ (curve b) electrodes to the successive addition of 10 μM catechol is shown in Fig. 4A. The electrocatalytic current of the bionanomultilayer electrode is three times higher than that of the electrode without MWNTs, which further confirms the function of the introduced MWNTs.

The typical amperometric response of the biosensor to successive addition of 0.4 μM catechol is shown in Fig. 4B. For each addition, a sharp increase of current is observed. Due to the MWNTs introduced into the bionanomultilayer, the current response of the biosensor reaches its maximum within 1 s. A calibration curve with linear range from 0.4 to 20.4 μM ($R = 0.9998$, $n = 51$) was obtained as shown in inset of the Fig. 4B. The detection limit (DL) of the biosensor was found to be 0.06 μM (S/N = 3), which was lower than the reported values (Liu et al., 2006; Yang et al., 2006).

3.4.2. Response of the biosensor to different phenolics

Table 1 presents the analytical performance of $(PAH\text{-}MWNTs/HRP)_5$ modified electrode including the sensitivity, linear range, correlation coefficient (R) and the detection limit

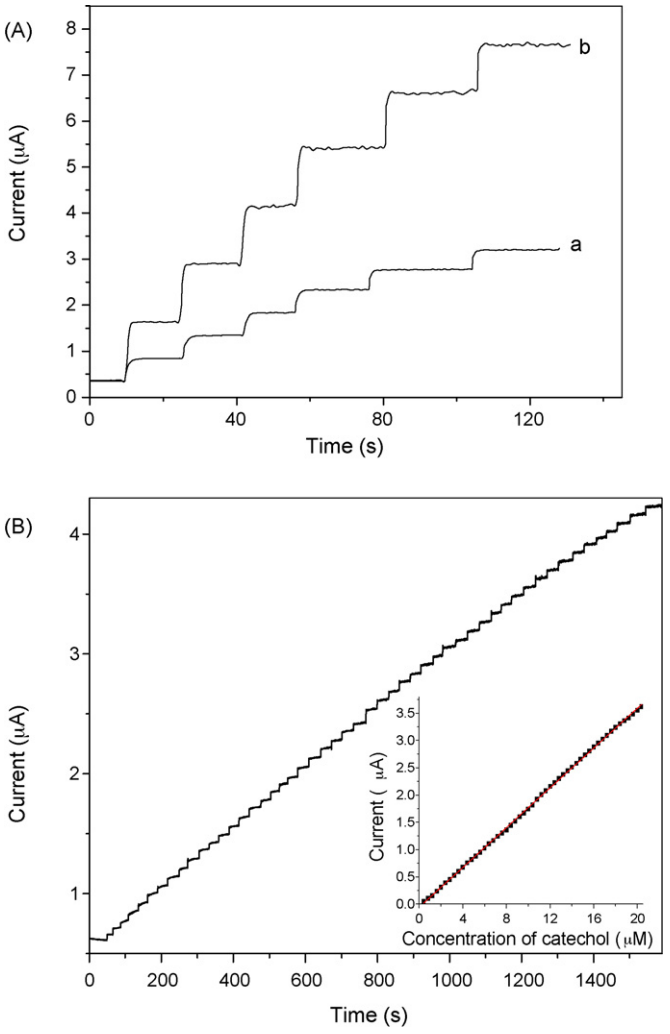

Fig. 4. The current response of (A) $(PAH/HRP)_5$ (a) and $(PAH\text{-}MWNTs/HRP)_5$ (b) modified electrode on successive addition of 10 μM catechol, and (B) the bionanomultilayer biosensor on successive addition of 0.4 μM catechol in present of 40 μM hydrogen peroxide in pH 6.5 PBS. Applied potential: −0.15 V. Inset is the calibration curve of the current response on the concentration of catechol.

(DL) for the compounds with different substituents including OH, NH_2, CH_3, Cl and NO_2. The polyphenol compounds, quercitrin and phytomelin, have the highest sensitivities. It can be attributed to the pyrone structure conjugated with the aromatic ring, which facilitates the oxidation to obtain corresponding quinone. The free electron on the resulting quinone radical is stabilized by the charge dissipation through the conjugated system. For the other compounds, it is clear that the type and position of the substituents have a strong influence on the sensitivity of the biosensor. The trends of the sensitivities for the phenolics are showed as follow: (1) *para*: *p*-aminopheno > hydroquinone > *p*-cresol > *p*-chlorophenol; (2) *ortho*: *o*-aminopheno > catechol > *o*-cresol > *o*-chlorophenol > *o*-nitrophenol; (3) *meta*: *m*-aminopheno > resorcinol > *m*-cresol > *m*-chlorophenol. It can be concluded that the sensitivity of different substituent phenolics follows the trend: $NH_2 > OH > CH_3 > Cl > NO_2$, which completely accords with the order of the electron donating ability of the substituents. The NO_2 substituent compounds except *o*-nitrophenol fail to generate any noticeable signal even after excessive additions, the reason of that is the electron withdrawing effect of the NO_2 group makes it difficult to form the free radical. Kane et al. have observed that the phenol compounds with electron-donor substituents in *ortho*-position have no response

Table 1
Analytical parameters of the biosensor for different phenolics

Phenolics	Structures	Sensitivity[a] (nA μM^{-1})	Linear range (μM)	*R*	DL (μM)
p-Aminophenol	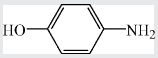	205	0.4–8.0	0.9996	0.05
o-Aminophenol		104	0.4–8.0	0.9989	0.07
m-Aminophenol	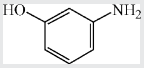	45.3	1.0–20.0	0.9990	0.2
Hydroquinone	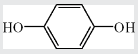	165	0.4–14.0	0.9994	0.05
Catechol		123	0.4–20.4	0.9998	0.06
Resorcinol	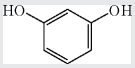	30.5	2.0–56.0	0.9991	0.1
p-Cresol	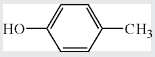	79.2	0.8–9.6	0.9976	0.09
o-Cresol	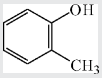	9.7	8.0–96.0	0.9963	1
m-Cresol	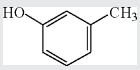	18.5	0.8–11.2	0.9984	0.3
p-Chlorophenol	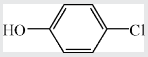	21.2	0.8–16.0	0.9992	0.2
o-Chlorophenol	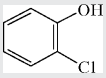	19.0	4.0–36.0	0.9918	0.8
m-Chlorophenol	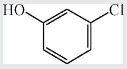	1.6	–	–	–
p-Nitrophenol	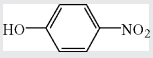	–	–	–	–
o-Nitrophenol	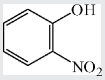	6.9	8.0–120.0	0.9892	2
m-Nitrophenol	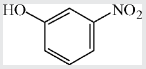	–	–	–	–
Quercitrin	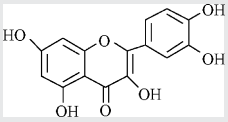	560	0.8–9.6	0.9992	0.1
Phytomelin	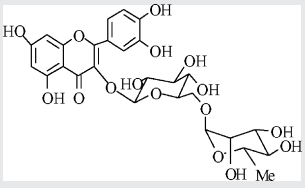	470	0.8–13.6	0.9994	0.08

[a] Obtained with 4.0 μM phenolics.

(Kane et al., 1998). But in our experiments, the electron-donor substituent compounds such as *o*-aminophenol (NH_2, *ortho*), catechol (OH, *ortho*) and *o*-cresol (CH_3, *ortho*) give strong responses. The sensitivity of the biosensor is higher than that of silica-based biosensor and CNT-based biosensor (Liu et al., 2006; Rosatto et al., 2002), which can be attributed to the MWNTs promoting the electron transfer and the LBL assembly offering a uniform film.

3.4.3. *Reproducibility and stability of the biosensor*

The reproducibility and stability are two important parameters for the evaluation of the performance of the biosensor. The repro-

ducibility of the same electrode, expressed as the relative standard deviation (R.S.D.), was less than 3.0%, which was obtained through nine successive experiments in the presence of 4.0 μM of catechol. The reproducibility of 10 electrodes was also examined and the R.S.D. was found to be 4.8%.

The stability of the multilayer electrode was evaluated by monitoring the response currents with 10 μM catechol over 90-day period. The electrode was stored at 4 °C in a refrigerator when not in use. The response was constant for the first 10 days. After 40 days, the response of the biosensor decreased to 93.4%. After 90 days of testing, the biosensor retained about 84.7% of its original response. The decrease of current response may be attributed to the denaturation of enzyme.

4. Conclusion

This study shows a novel water-soluble PAH-MWNTs in barbiturate solution, which can be used to construct the $(\text{PAH-MWNTs/HRP})_n$ bionanomultilayer through LBL assembly. The bionanomultilayer exhibits a highly uniform and homogeneous characteristic. The developed biosensor based on the bionanomultilayer can be successfully applied to determination a series of phenolics. Attribute to the introduced MWNTs, the biosensor exhibits a quick, sensitive and stable detection. Furthermore, the water-soluble CNTs and the bionanomultilayer offer a useful avenue for application of CNTs into the material science and biosensor fields.

Acknowledgements

Financial support from the Zhejiang Provincial Natural Science Foundation (Project No. 2007-Z406180) is acknowledged. L.J. Liu gratefully acknowledges the support of Jinggangshan University, PR China.

References

Ajayan, P.M., 1999. Chem. Rev. 99, 1787–1799.
Ali, S.R., Ma, Y., Parajuli, R.R., Balogun, Y., Lai, W.Y.-C., He, H., 2007. Anal. Chem. 79, 2583–2587.
Baughman, R.H., Zakhidov, A.A., de Heer, W.A., 2002. Science 297, 787–792.
Chen, J., Hamon, M.A., Hu, H., Chen, Y., Rao, A.M., Ehlund, P.C., Haddon, R.C., 1998. Science 282, 95–98.
Chen, L., Lu, G., 2007. Sens. Actuator B: Chem. 121, 423–429.
Cosnier, S., 2003. Anal. Bioanal. Chem. 377, 507–520.
Deo, R.P., Wang, J., Block, I., Mulchandani, A., Joshi, K.A., Trojanowicz, M., Scholz, F., Chen, W., Lin, Y.H., 2005. Anal. Chim. Acta 530, 185–189.
Georgakilas, V., Tagmatarchis, N., Pantarotto, D., Bianco, A., Briand, J.P., Prato, M., 2002. Chem. Commun., 3050–3051.
Jiang, X.M., Chen, Z.C., Yang, S.M., Lin, H.F., Lin, X.F., 2004. Chin. Chem. Lett. 15, 547–550.
Kane, S.A., Iwuoha, E.I., Smyth, M.R., 1998. Analyst 123, 2001–2006.
Liu, G.D., Lin, Y.H., 2006. Anal. Chem. 78, 835–843.
Liu, J., Rinzler, A.G., Dai, H., Hafner, J.H., Kelley-Bradley, R., Boul, P.J., Lu, A., Iverson, T., Shelimov, K., Huffman, C.B., Rodriguez-Macias, F., Shon, Y.-S., Randall Lee, T., Colbert, D.T., Smalley, R.E., 1998. Science 280, 1253–1256.
Liu, Y., Qu, X.H., Guo, H.W., Chen, H.J., Liu, B.F., Dong, S.J., 2006. Biosens. Bioelectron. 21, 2195–2201.
Mello, L.D., Sotomayor, M.D.P.T., Kubota, L.T., 2003. Sens. Actuator B: Chem. 96, 636–645.
Munteanu, F.D., Lindgren, A., Emneus, J., Gorton, L., Ruzgas, T., Csoregi, E., Ciucu, A., Van Huystee, R.B., Gazaryan, I., Langrimini, L.M., 1998. Anal. Chem. 70, 2596–2600.
O'Connell, M.J., Boul, P., Ericson, L.M., Huffman, C., Wang, Y., Haroz, E., Kuper, C., Tour, J., Ausman, K.D., Smalley, R.E., 2001. Chem. Phys. Lett. 342, 265–271.
Pompeo, F., Resasco, D.E., 2002. Nano Lett. 2, 369–373.
Rosatto, S.S., Sotomayor, P.T., Kubota, L.T., Gushikem, Y., 2002. Electrochim. Acta 47, 4451–4458.
Sampath, S., Lev, O., 1996. Anal. Chem. 68, 2015–2021.
Star, A., Steuerman, D.W., Heath, J.R., Stoddart, J.F., 2002. Angew. Chem. Int. Ed. 41, 2508–2512.
Wang, J., 2005. Electroanalysis 17, 7–14.
Wang, J., Musameh, M., 2003. Anal. Chem. 75, 2075–2079.
Wu, F.H., Zhao, G.C., Wei, X.W., 2002. Electrochem. Commun. 4, 690–694.
Yan, X.X., Pang, D.W., Lu, Z.X., Lu, J.Q., Tong, H., 2004. J. Electroanal. Chem. 569, 47–52.
Yang, S.M., Chen, Z.C., Jin, X., Lin, X.F., 2006. Electrochim. Acta 52, 200–205.
Zhang, M., Yan, Y., Gong, K., Mao, L., Guo, Z., Chen, Y., 2004. Langmuir 20, 8781–8785.
Zhao, Q., Gan, Z., Zhuang, Q., 2002. Electroanalysis 14, 1609–1613.